Astron. Astrophys. 356, 1076–1088 (2000)

ASTRONOMY AND ASTROPHYSICS

Physical properties of TNO 1996 TO_{66}⋆

Lightcurves and possible cometary activity

O.R. Hainaut[1], **C.E. Delahodde**[1], **H. Boehnhardt**[1], **E. Dotto**[2,3], **M.A. Barucci**[2] **K.J. Meech**[4], **J.M. Bauer**[4], **R.M. West**[5], **and A. Doressoundiram**[6]

[1] European Southern Observatory, Casilla 19001, Santiago, Chile
[2] Observatoire de Paris, DESPA, 5, Place Jules Janssens, 92190 Meudon Principal CEDEX, France
[3] Osservatorio Astronomico di Torino, Strada Osservatorio 20, 100025 Pino Torinese (TO), Italy
[4] Institute for Astronomy, 2680 Woodlawn Drive, Honolulu, Hawaii 96822, U.S.A.
[5] European Southern Observatory, Karl-Schwarzschild-Strasse 2, 85748 Garching bei München, Germany
[6] California Institute of Technology, Jet Propulsion Laboratory, 4800 Oak Grove Drive, Pasadena, CA 91109, USA

Received 1 June 1999 / Accepted 13 January 2000

Abstract. We describe observations of the Trans-Neptunian Object (TNO) 1996 TO_{66} performed during three observing runs (August 1997, October 1997 and September 1998). They show significant brightness variations that indicate a rotation period of 6.25 ± 0.03h. In the the 1997 data, the phased lightcurve displays a nearly symmetrical double peak with a peak-to-peak amplitude of 0.12 mag, while in the data of 1998, it shows a single maximum with a full amplitude of 0.33 mag. Possible causes for this change of shape are explored, the simplest explanation being that 1996 TO_{66} experienced a phase of cometary activity during the interval between these observations. This hypothesis, if confirmed, could be of interest for the pending question of the observed color diversity of TNOs.

The average magnitude ($R = 21.15$) was converted into a mean radius of 326 ± 7 km (assuming albedo $p = 0.04$), making 1996 TO_{66} the largest known TNO after Pluto and Charon. The object is among the bluest in the outer Solar System and the colour, as measured at different epochs, shows marginally significant changes. Deep, composite images, totaling 13,500s integration time with the NTT and 4500s with the UH 2.2m in the R filter, were searched for possible signatures of a faint coma. None were found and the photometric profile of 1996 TO_{66} perfectly matches a stellar one, down to the 29 mag/sq.arcsec level. We also present an apparently featureless 8100s NTT +EMMI spectrum (6000-9100Å) with a neutral reflectivity in the 6000–7600Å range, and with a marginally significant red gradient $S' = 30 \pm 10\%$/1000Å in the 7600–9000Å range.

Key words: Kuiper belt, Oort cloud – planets and satellites: individual: 1996 TO66 – solar system: formation

Send offprint requests to: O.R. Hainaut, ESO-Chile

⋆ Based on observations collected at the European Southern Observatory, La Silla, Chile, and University of Hawaii Telescope, Mauna Kea, Hawaii, USA.

1. Introduction

More than 200 Trans-Neptunian Objects (TNOs) have been found since the discovery in 1992 of the first of this class (not counting Pluto), 1992 QB1 (Jewitt & Luu 1992). The measured magnitudes are in the $R \sim 21-26$ range, and it is assumed that they represent a sample of the brightest members of this new class of Solar System objects. It is estimated (Jewitt 2000) that at least 100,000 TNOs with diameters larger than 100 km move in nearly circular orbits at heliocentric distances between $r \sim 30$ and 50 AU. They populate three broad dynamical classes: *i)* classical Kuiper Belt objects (orbits with low inclination and eccentricity), *ii)* "Plutinos" (like Pluto, in orbital 2:3 resonance with Neptune), and *iii)* "Scattered TNOs" with highly elliptical and inclined orbits, due to gravitational interaction with Neptune. The latter class was recognized after the discovery of 1996 TL_{66} (Luu et al. 1997) that moves in a high-eccentricity orbit between $r \sim 35$ and 130 AU. It is currently speculated that a "wall" of TNOs may be found beyond $r \sim 70-90$ AU (cf. Trujillo 2000 for simulations). At these and larger heliocentric distances, gravitational perturbations by the major planets are negligible, and the objects in that region would have survived since their formation in quasi-stable orbits, thus constituting an important reservoir of primitive remnants from the early accretion phases of the Solar System (Malhotra 1996, 1997). This scenario represents the contemporary version of the original ideas about icy objects in the outer Solar System (*i.e.* beyond Neptune), first published by Edgeworth (1943) and Kuiper (1951). Also, recent observations of proto-planetary disks frequently show abrupt cut-offs in the radial surface density of the dust disk at a distance smaller than 100 AU from the star, most likely due to a large number of neighborhood stars (McCaughrean 2000; Kalas 2000). If the TNO density abruptly drops in the $r > 50$ AU region, one may have to consider that the Solar System proto-planetary nebula was more similar to these cut-off disks than to that of β Pictoris.

Because of the faint TNO magnitudes and instrumental limitations, it is only now becoming possible to initiate systematic

observational studies of the physical nature of these objects, flanked by appropriate theoretical efforts. For the time being, only the most important issues can be addressed in any detail, e.g., the establishment of a rough classification scheme for these objects and a first exploration of how they relate to other Solar System bodies. It appears likely that TNOs, Centaurs and periodic comets constitute different evolutionary steps of a gravitational cascade that transports icy objects from the near Trans-Neptunian region (25–45 AU) into the inner Solar System. In this context, it is indispensable to obtain a solid basis of high-quality data at the limit of what is possible with existing telescope and instrument equipment, providing information about size and shape, rotational state, colours and albedo, surface chemistry, structure and possible activity of a statistically significant sample of TNOs.

The observational approach for such studies uses both short-term runs on a larger subset of TNOs, e.g., for colour and size estimates, as well as longer campaigns aimed at the detailed investigation of individual objects and the measurement of their shape, rotation and spectral signatures of the surface and/or possible surrounding atmosphere. Theoretical considerations indicate that the surface properties of TNOs may be modified by alteration processes *i)* through the interactions with the high energy particle and radiation environment in space (Sagan et al. 1984), *ii)* through erosion and collisions with dust and smaller chunks, occasionally also with other planetesimals (Stern 1996; Davis & Farinella 1997) and *iii)* through cometary activity, some comets being still active at $r \sim 25$ AU, *i.e.* not too far from the region where the known TNOs reside (Meech & Hainaut 1997). Moreover, evolution of the interior seems to be possible for bodies as small as ∼100km (Prialnik et al. 1987; Prialnik & Bar-Nun 1990; Prialnik 2000), which may have an impact on the generation of continuing surface activity on TNOs. It appears that erosion generally dominates over accretion, leading to questions on how the observed bodies were formed. Collisions have been shown to play a substantial role in the Edgeworth-Kuiper Belt (EKB), especially in the inner part of this region (Farinella & Davis 1996; Davis & Farinella 1997). Thus, knowledge of rotational properties is important for the investigation of accretion processes and the collisional evolution of the population.

The available observational studies of the physical characteristics of TNOs are based on photometry and spectroscopy in the visible and near-infrared regions. Spectra have been published for only three TNOs: 1993 SC (visible: Luu & Jewitt 1996, near-IR J band: Brown et al. 1997), 1996 TL_{66} (visible and near-IR: Luu & Jewitt 1998), and 1996 TO_{66} (near-IR spectrum showing the signature of H_2O, Brown et al. 1999; this result will be discussed below). The spectra are different, implying different surface composition. Tegler & Romanishin (1998) found, on the basis of B, V and R data for 11 TNOs and 5 Centaurs, that the TNO and Centaur population is split in two distinct groups: one of neutral colours and one that is very red. However, by comparing all the broadband colours available to date (22 objects), Barucci et al. (1999) found a complex and non-homogeneous population composition, with no evidence of the two mentioned groups (their colour diagrams are shown in Fig. 2). While these early results imply a certain degree of diversity and hence different evolutionary stages or paths already in the present, small TNO sample, it is also obvious that this young research field is now in an initial state that can only progress by means of additional and accurate observations of a much larger sample.

In this paper we present a detailed study of 1996 TO_{66}, a "classical Kuiper Belt" TNO in a quasi-circular (eccentricity $e = 0.11$), medium inclination ($i = 27.3°$) orbit at a mean solar distance of about 45 AU. The observations were obtained during three observing periods in 1997 and 1998 and aimed at the determination of the size and shape, the rotation and the colours of this object, as well as a deep search for a coma and spectral signatures from surface or coma species. The observations are described in the next section. The results are presented and discussed in Sect. 3.

2. Observations and data processing

2.1. Observations

Observations of 1996 TO_{66} for the present study were obtained during three runs. The first, on Aug. 27 and 28, 1997, used the SuSI CCD camera at the "A" f/11 Nasmyth focus of the 3.6m ESO New Technology Telescope (NTT) on La Silla, Chile to obtain direct images with a Bessel V filter. The second run took place on Oct. 21–25, 1997, also at the NTT, but with the EMMI-RILD camera ("ESO Multi-Mode Instrument", in "Red Imaging and Low Dispersion" mode), on the "B" focus. During the first four nights of this run, the first half of the night was spent on taking many Bessel R images and a few through the Bessel B, V, and I filters (during 3 of the nights). The last night was mostly devoted to obtaining eight 900 sec exposure spectra of 1996 TO_{66}, using the EMMI-RILD instrument with a slit of 2″ and Grism #4 (300 lines/mm, giving a dispersion of 2.8 Å/pix over the 5650–10000 Å range, resulting in a spectral resolution of $R \sim 380$ for a 2″ slit, although we degraded this resolution during the data processing in order to increase the signal-to-noise ratio).

A secondary purpose of Run 2 was to perform a "pencil-beam" search for very faint and/or very distant Solar System objects. The results of this search are presented elsewhere (Böhnhardt et al. 2000).

The third run took place on Sep. 26–28, 1998. The University of Hawai'i 2.2m telescope (UH88"), on Mauna Kea Observatory (MKO), Hawai'i, was used with the Direct Imaging Camera equipped with Kron-Cousin filters.

Table 1 lists the technical description of the instruments, as well as the observers and meteorological conditions during the three runs. Table 2 lists the parameters of the filters used on the different instruments.

During all three runs, the telescope was guided at sidereal rate. For Run 2, the exposure time of the imaging frames was 900s, resulting in a trailing of the moving object of ∼0.″6, *i.e.* of the order of, or slightly smaller, than the actual seeing (0.6–1.″1 FWHM). For Runs 1 and 3, the exposure time was 300s, so that

Table 1. Observation Circumstances

Night	Telescope	Instrument			Observers	Weather
		Name	Detector	Pix.		
Run 1						
1997-Aug-27	ESO	SuSI-1	TK 1024M4	0.125	MAB	Photometric
1997-Aug-28	3.6m NTT		(ESO#25)		MAB	Photometric
Run 2						
1997-Oct-21	ESO	EMMI-RILD	Tek 2048EB 2	0.270	HBO, ORH	Cirrus, alto-cumulus
1997-Oct-22	3.6m NTT		(ESO#36)		HBO, ORH	Cirrus, alto-cumulus
1997-Oct-23					HBO, ORH	Photometric
1997-Oct-24					HBO, ORH	Photometric
1997-Oct-25					HBO, ORH	Photometric
Run 3						
1998-Sep-26	MKO	Direct	Tek 2048	0.219	KJM, JBA	Thin and stable cirrus
1998-Sep-27	2.2m UH				KJM, JBA	Thin and stable cirrus
1998-Sep-28					KJM, JBA	Photometric, except 30min

Notes: "Night" lists the UT date of the beginning of night. Instrument: SuSI-1 = Superb Seeing Imager 1, EMMI-RILD = ESO Multi-Mode Instrument in Red Imaging and Low Dispersion mode. Pix. is the pixel scale in arcseconds. Observers: MAB= M.A. Barucci, HBO= H. Böhnhardt, ORH= O.R. Hainaut, KJM= K.J. Meech, JBA= J. Bauer.

Table 2. Parameters of the filters

Filter	λ_c	FWHM
Run 1: SuSI		
Bessel B #639	434.0	101.1
Bessel V #641	547.2	113.3
Bessel R #642	643.8	166.7
Run 2: EMMI		
Bessel V #606	542.0	105.0
Bessel R #608	645.0	155.0
Bessel I #610	800.0	158.0
Run 3: UH Direct Camera		
Kron-Cousin B	438.0	107.7
Kron-Cousin V	545.0	83.6
Kron-Cousin R	646.0	124.5
Kron-Cousin I	826.0	188.8

the trailing would be small ($\sim 0\farcs2$) compared to the seeing (0.6–$1\farcs1$ and 0.5–$0\farcs7$ FWHM for Run 1 and 3 resp.). The telescopes were dithered between each exposure to allow us to build some "super-flats" from the frames themselves, and to minimize the impact of bad pixels and bad columns. Table 3 lists the positions and the geometric parameters of the object for each night.

During the photometric nights, various Landolt (1992) fields were observed at different airmasses, allowing a direct determination of the extinction coefficients and thus to perform a complete photometric transformation (zero points and colour terms).

In order to calibrate the spectroscopic data during Run 2, spectra were acquired of LTT3218, a spectrophotometric standard (Hamuy et al. 1992, 1994), and of HD30455, a solar analog, in addition to He-Ar lamp exposures for wavelength calibration and spectroscopic dome flat-fields.

2.2. Data processing

2.2.1. Direct imaging

Bias and Flat field: A 2D bias template, obtained by averaging many 0-sec exposures, was subtracted from each frame. The procedures used for the 3 runs are different, but each of them either subtract from the images the residual mean value of the bias-subtracted overscan, and/or checks that this value is negligible. The dark current of the used CCDs was checked and found negligible, and was accordingly not corrected for. The sensitivity variations across the field of view were removed by dividing the frames by a flat-field constructed from spatially offset frames of the twilight sky. In the case of Run 2, the flat-field was further improved by using a composite of the dome and twilight flats, and of the scientific frames themselves, by means of a wavelet transform combination technique, described in the paper by Hainaut et al. (1998). The data processing was performed using MIDAS and IRAF software packages.

Photometric calibration: The instrumental magnitudes were measured using aperture photometry (PHOT task in IRAF Digiphot package, and a procedure based on MAGNITUDE/CIRCLE in MIDAS), by means of a small aperture in order to minimize the sky noise. For Run 1, a diaphragm of $3\farcs8$ in diameter (12 pix) was typically used, for Run 2, $5''$ diameter, and $2\farcs6$ (12 pix) for Run 3. Considering the actual seeing during the latter, the diaphragms then used is expected to contain all but at most 4% of the light from 1996 TO_{66}; no correction was made for this effect. An integrated magnitude *vs* diaphragm diameter plot for these data actually show that we are missing only 1.6% of the light, *i.e.* even less than the estimate obtained directly from the comparison between the seeing disk and the diaphragm. For the other runs, the diaphragm was considerably larger than the seeing. In order to verify this, the magnitude of several brighter objects was measured through a series of

Table 3. Ephemerides for 1996 TO_{66}

Epoch (UT)	α_{2000}	δ_{2000}	$\dot{\alpha}$ [″/h]	$\dot{\delta}$ [″/h]	r [AU]	Δ [AU]	$\alpha_{\rm phase}$ [deg]	θ [deg]
1997-Aug-27 05:00	23 56 19.33	+02 02 05.2	-2.47	-0.76	45.755	44.845	0.56	153.91
1997-Aug-28 05:00	23 56 15.44	+02 01 46.9	-2.49	-0.77	45.755	44.838	0.54	154.89
1997-Oct-21 02:00	23 52 37.38	+01 43 05.1	-2.35	-0.84	45.775	44.900	0.59	151.25
1997-Oct-22 02:00	23 52 33.39	+01 42 43.4	-2.33	-0.83	45.775	44.910	0.61	150.16
1997-Oct-23 02:00	23 52 29.75	+01 42 23.6	-2.30	-0.82	45.775	44.919	0.63	149.15
1997-Oct-24 02:00	23 52 26.16	+01 42 04.0	-2.27	-0.81	45.776	44.928	0.65	148.15
1997-Oct-25 02:00	23 52 22.62	+01 41 44.7	-2.24	-0.80	45.776	44.938	0.67	147.14
1998-Sep-26 10:00	23 57 10.96	+02 45 13.1	-2.76	-0.95	45.856	44.856	0.08	176.13
1998-Sep-27 10:00	23 57 06.63	+02 44 50.3	-2.75	-0.95	45.857	44.857	0.10	175.38
1998-Sep-28 10:00	23 57 02.31	+02 44 27.5	-2.75	-0.95	45.857	44.859	0.11	174.55

Notes: The equatorial coordinates (J2000.0) and motions are listed for the mean epoch of the observations (local midnight for Runs 1 and 3, 1st quarter of the night for Run 2). $\alpha_{\rm phase}$ is the solar phase angle, and θ is the solar elongation. Information is from the JPL Solar System Dynamics Service.

diaphragms with diameters in the 0.1–15″ range. Plots of the resulting magnitudes as a function of the diaphragm diameter confirm that the magnitudes obtained with the diaphragm used in this paper are already far into the asymptotic regime, thus indicating that the light lost in the wings of the PSF outside the diaphragm is negligible. These tests and other simulations will be discussed in detail in a paper by Delahodde et al. (2000).

It should be additionally noted that, as we used apertures of constant diameters, the variations of seeing formally introduced small changes in the fraction of the light that is not taken into account in the measurement. However, as the aperture is significantly larger than the seeing, these variations are at the $<<1\%$ level, and therefore much smaller that the other sources of error. These variations must be taken into account when using very small apertures, as described in Tegler & Romanishin (1998), and references therein.

The sky was measured in an annulus centered on the object, extending typically from 5 to 10 arcsec from the center, as a $\kappa\sigma$ clipped average of the background. This ring, as well as the "no man's land" between the diaphragm and the sky ring, were individually adjusted in order to avoid field star contamination.

As mentioned above, Bessel filters were used during Runs 1 and 2, and Kron-Cousin's filters during Run 3, but all runs were calibrated by means of photometric standards from the same system (Bessel), as the R filter transmission curves of both systems are very similar. As 1996 TO_{66} was found to have a smooth, fairly neutral spectrum in the corresponding wavelength interval (cf. Sect. 3.5), any magnitude errors introduced by the use of this hybrid system are negligible in comparison to the other sources of errors; they were consequently not taken into account in this discussion.

The instrumental magnitudes were converted into apparent magnitudes using the zero point, extinction and colour terms obtained from the Landolt fields for each filter. However, as some of the Run 2 and 3 nights were non-photometric, such magnitudes cannot be used directly: they will be corrected for the absorption by differential photometry.

Differential Photometry: Many field stars were measured on each frame (e.g. 45 for Run 2, 20 for Run 3). Due to the slow motion of 1996 TO_{66}, the same field stars could be observed during all the nights of each run. Their average magnitudes, as measured during the photometric nights, were used to perform relative photometry. This ensured an excellent correction of all extinction variations caused by the passing of clouds, and for second order extinction variations. In the case of cirruses, the actual corrections were always smaller than 0.1 mag. In order to demonstrate the efficiency of these corrections, the corrected magnitudes of the object and of reference stars of similar magnitude are displayed in Fig. 1. The remaining variations for the stars are smaller than 0.01 mag.

2.2.2. Spectroscopy

The individual spectral frames were bias subtracted. The spatial sensitivity map was corrected for by using a flat-field built from a series of spectral dome exposures: the average spectrum of the lamp was removed from the average of the normalized flat-field frames. The spectral data processing was performed by means of the MIDAS LONG package. All 2D-spectra were calibrated in wavelength and rebinned with uniform wavelength bins using a 3^{rd} degree dispersion law obtained from the He-Ar exposure. 1D spectra were then extracted by fitting on each column of the images (*i.e.* for each wavelength along the spatial direction) a linear continuum (representing the sky) and a gaussian representing the object. The integrated flux of these gaussians are kept as a function of the wavelength, forming the individual spectra. This technique has the advantage to use optimally the whole flux of the object over the whole seeing and perfectly model the underlying sky. Additionally, it takes perfectly into account the curvature of the spectrum caused by the atmospheric differential refraction. As the actual instrumental profile is not a perfect gaussian (but closer to a moffat, *i.e.* a gaussian with low, fat wings), this technique underestimates the flux in each wavelength bin by $\sim 5\%$. We verified that this effect does not depend on the flux nor the wavelength of the object. As we pro-

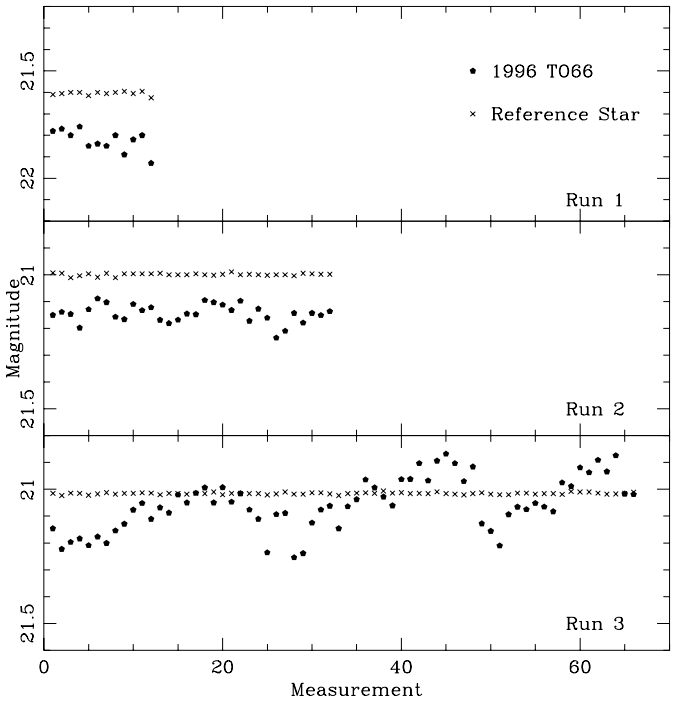

Fig. 1. Magnitude of 1996 TO_{66} (dots) and of comparison stars of similar magnitude (x), for the 3 runs, after correction by differential photometry. The abscissa of the plots is the measurement sequence number (not the epoch). This figure demonstrate that the object's magnitude variations are much larger than the residual errors of the differential photometry.

cess the spectra in a relative way with respect to the standard star and solar analog, whose spectra were extracted in the same way, this effect is of no consequence. The spectral response of the instrument was determined by comparing the spectrum of the spectrophotometric standard with the flux tabulated in MIDAS, and applying the site specific wavelength dependence of the extinction. All 1D spectra were flux calibrated using the resulting response curve and the standard extinction. Finally, the spectra of 1996 TO_{66} were stacked and smoothed using a sliding median filter with a window of 5 pix, and rebinned to 20Å bins to reduce the noise. The spectrum presented in Fig. 7 has been divided by that of the solar analogue in order to produce a reflectance spectrum.

3. Results

3.1. Radius

We adopted for 1996 TO_{66} the canonical cometary surface albedo of 0.04 (P/Halley), which is further confirmed for TNOs by the thermal IR measurements obtained with ISO (Thomas et al. 2000), and neglected the very small solar phase effects (Table 3). The average magnitude of 1996 TO_{66} from each run was converted into a mean radius (Russell 1916).

The data were obtained at very small phase angle, *i.e.* where an opposition surge is expected in the phase curve. However, as the phase curve of such an object is totally unknown, we cannot take it into account properly. Assuming that the surface of 1996 TO_{66} behaves like that of a comet, the theoretical work of Bowell et al. (1989) and its application to the observations of Comet P/Encke's nucleus by Luu & Jewitt (1990) show that a phase coefficient $\beta \simeq 0.04$mag/deg is reasonable for phase angles in the range from 5 to $\sim 100°$, but that an opposition surge of 0.2mag at least is possible for very small angles. Instead of correcting for this unknown effect, we prefer to present the data without any phase correction. As our data were taken in the $\alpha = 0.08$–$0.67°$range, the opposition surge could modify the phase corrected magnitudes by as much as 0.1 mag.

Table 4. Average Radius of 1996 TO_{66}

Run	Band	Mag	M(1,1)	r [km]
1	V_b	21.84 ±0.06	5.28	300.
2	R_b	21.15 ±0.05	4.59	326.
3	R_{kc}	21.05 ±0.05	4.48	340.
1997 Sep. 23/24	V	21.40 ±0.03	4.52	
(JL98)	R	21.08 ±0.05		
1997 Oct. 3-6	V	21.38 ±0.05	4.75	380.
(RT99)				

Notes: V_b and R_b refer to the Bessel filters, R_{kc} to that in the Kron-Cousin system; M(1,1) is the corresponding absolute magnitude. The second part of the table lists the magnitudes and radii published by Jewitt and Luu (1998) and Romanishin and Tegler (1999) as comparisons.

Unless the albedo value is much higher than here assumed, 1996 TO_{66} is one of the largest known TNOs, in fact the largest so far identified, apart from Pluto (radius = 1200km) and Charon (600km). Its surface may possibly more resemble that of the planet or its satellite than that of a cometary nucleus.

3.2. Colours

Table 5 lists the colours of 1996 TO_{66}, as determined during the present runs. For Run 2, the other filters were measured alternatively with the R filter, in order to estimate the possible changes of cross-section caused by rotation. For each filter, the R magnitude has been interpolated for the corresponding epoch from temporally adjacent R measurements; the colours obtained should therefore be free of any rotation effect. The colours relative to R have been combined into the traditional colour indices, which are listed in Table 5, together with colors from other authors, for comparison.

In Fig. 2, the measured colour indices of 1996 TO_{66} are plotted in $(V-R)$, $(B-V)$ and $(R-I)$ colour diagrams, together with those of other outer Solar System minor bodies measured by Barucci et al. (1999). It is obvious that 1996 TO_{66} is among the bluest known in this population. Compared to the solar colours, those of 1996 TO_{66} range from slightly blue ($B-V$ and $V-R$) to neutral ($R-I$).

Primitive outer Solar System materials are believed to be mostly constituted of ices mixed with carbon and simple hydrocarbon molecules, lending them a dark grey colour. Lab-

Table 5. Colour indices of 1996 TO_{66} (free of rotation effect). Colors of the object found in the literature have been listed for comparison.

Date	$B-V$	$V-R$	$R-I$	Ref.
1997-Oct-21 0.3–2.1	0.69±0.06	0.34±0.04	0.31±0.08	
1997-Oct-23 1.7–3.9	0.56±0.07	0.44±0.05	0.37±0.07	
1997-Oct-25 6.0–6.5	0.62±0.07	0.44±0.05	0.49±0.06	
1998-Sep-27 6–9		0.28±0.05	0.34±0.06	
1998-Sep-28 6–9		0.39±0.05	0.41±0.06	
1997(?)	0.74±0.04	0.38±0.03		TR
1997-Sep-24	0.59±0.06	0.31±0.06	0.36±0.07	JL

Reference: TR = Tegler and Romanishin (1998), JL = Jewitt and Luu (1998)

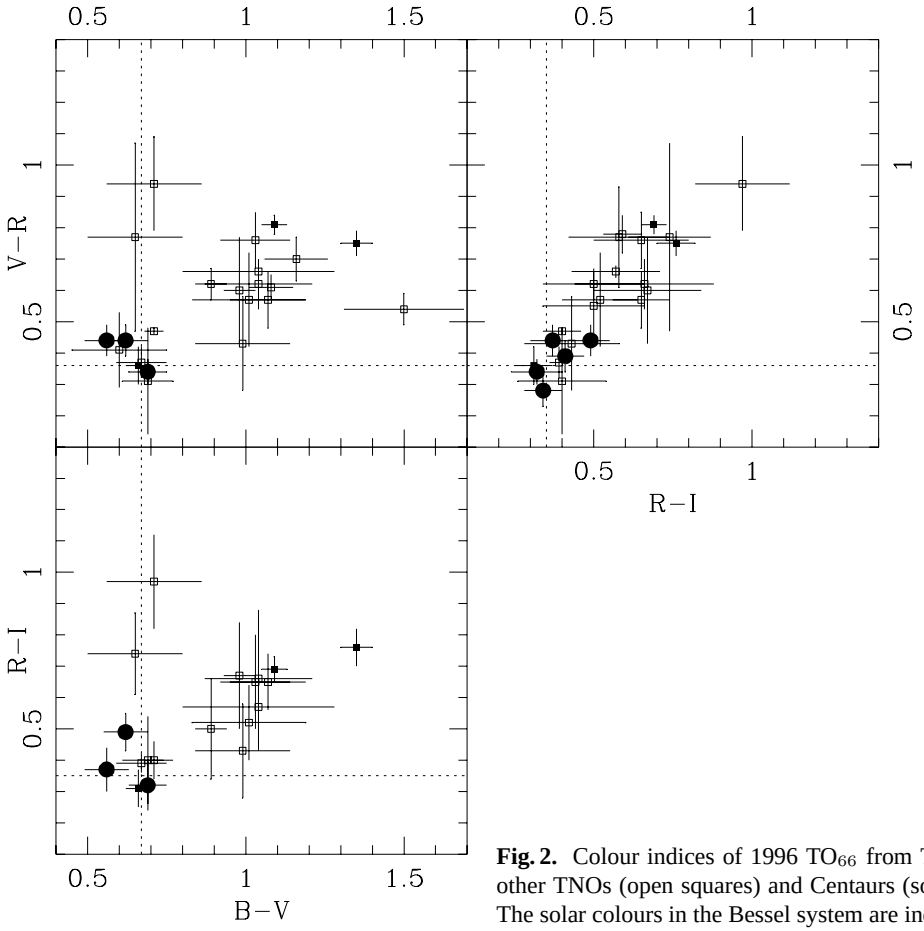

Fig. 2. Colour indices of 1996 TO_{66} from Table 5 (solid circles), compared with several other TNOs (open squares) and Centaurs (solid squares), both from Barucci et al. , 1999. The solar colours in the Bessel system are indicated by dotted lines

oratory experiments (Sagan et al. 1984) show that irradiating these material with high-energy photons (representing the stellar UV radiation and cosmic rays) produces large hydrocarbon molecules. The resulting mixture (known as *tholin*) has a dark, very red colour (Johnson et al. 1987; Moroz et al. 1998). The grey colour of some TNOs, including 1996 TO_{66}, may be interpreted in different ways. One possibility is that the objects have been re-surfaced by impacts, which excavate some of the primitive (grey) material from the interior and distribute it over the surface where it would then become affected by the reddening process. While this model can account for the continuous distribution of colour reported by Barucci et al. (1999), it fails to explain the dual distribution presented by Tegler & Romanishin (1998), in which all the objects they observed are clumped into two regions of the $(V-R) vs. (B-V)$ diagram ($(B-V)$ in 0.6–0.8, $(V-R)$ in 0.3–0.5 for the first region, and 1.0–1.3,0.6–0.8 for the second). According to this model, the measured colours of 1996 TO_{66} indicate that it would have been re-surfaced very recently, possibly by one major impact or a series of minor impacts which would have re-coloured most of the surface. Nevertheless, simulations of the time scale for such impacts (Stern 1995) suggest that their frequency is too low to explain this kind of resurfacing as a general feature of TNOs.

Another promising hypothesis is that the resurfacing would be caused by cometary activity. Indeed, (2060) Chiron's

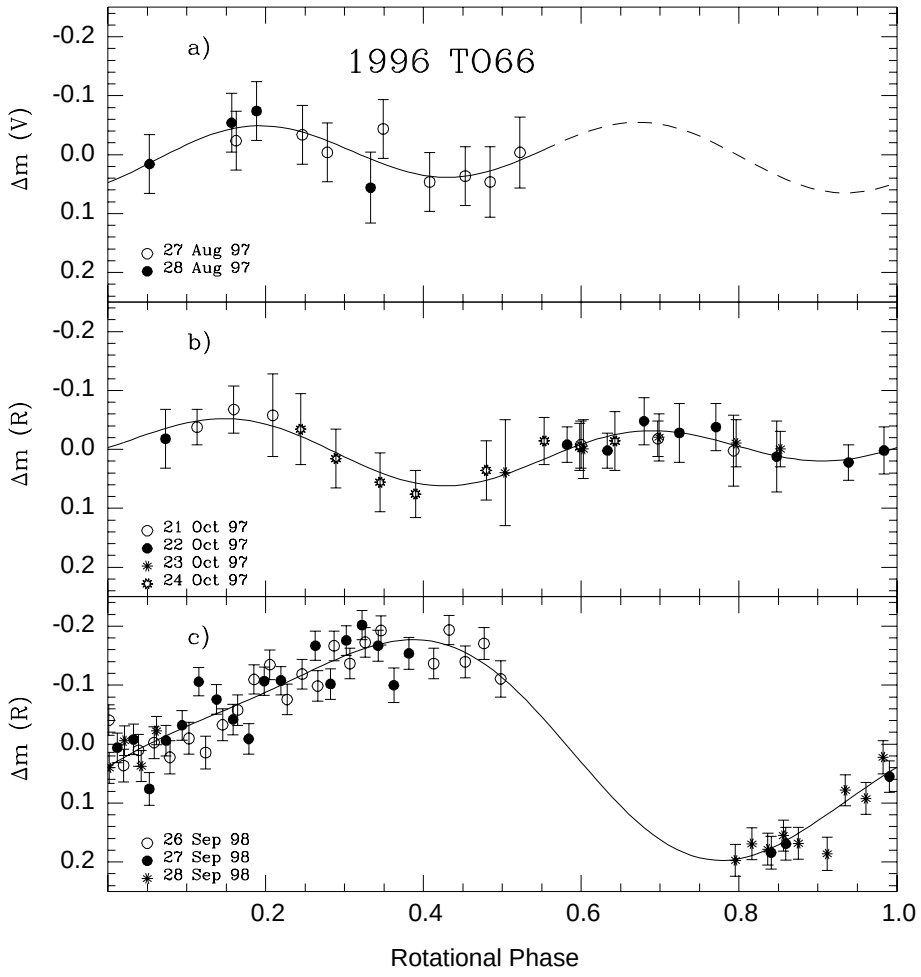

Fig. 3. Phased lightcurves of 1996 TO_{66}, folded with $P_{\rm syn} = 6.25$h. The line represents the modeled lightcurve, as computed by the period searching program. The error bars include the photon noise as well as the photometric calibration error. The data from all three runs were phased using the 6.25 h period. The actual origins for the phases are 1997 August 28.0 for Run 1, 1997 October 22.940 for Run 2 (an integer multiple of periods after the origin for Run 1) and 1998 September 27.0 for Run 3.

surface, which is known to be active, presents blue-grey colours similar to those of 1996 TO_{66}, as do the nuclei of comets 24P/Grigg-Skjellerup and 63P/Schwassmann-Wachmann 3 (Böhnhardt et al. 1999). This possibility is further investigated in the following sections on the basis of the present observations.

3.3. Lightcurve

3.3.1. Results

Very few TNO lightcurves have been published; most of them are either too noisy and/or not well enough sampled to allow the lightcurve parameters to be derived, cf. the review by Davies (2000). Most notably, a possible period of ∼10h has been reported for 1994 VK_8 and of ∼8h for 1995 QY_9 (Romanishin & Tegler 1999), both with fairly large amplitudes, 0.4 and 0.6 mag, respectively. Three Centaurs have published rotation periods: (2060) Chiron (5.9h), (5145) Pholus (10.0h) and (8405) 1995 GO (8.9h – refer to the paper by Davies (2000) for details and references).

The present data for 1996 TO_{66} show some significant variations with time. Good time coverage and sampling was obtained during each run; these data therefore lend themselves to a detailed analysis of the lightcurve. A period search was performed on the data of Runs 1 and 2, using an algorithm derived from that of Harris & Lupishko (1989). The only period that matched the observations from both runs, both individually and together (*i.e.* without adjusting the phase of one of the run with respect to the other), is $P_{\rm syn} = 6.25$h. This corresponds to 215 full rotations between Runs 1 and 2. The periods corresponding to 214 and 216 rotations (*i.e.* 6.275h and 6.218 h) clearly do not fit the data. We conclude that the uncertainty on P_{syn} is smaller than half the difference between these periods and adopt, as the best fitting period, $P_{\rm syn} = 6.25 \pm 0.03$h.

The phased magnitudes are displayed in Fig. 3. It should be noted that two points from Run 1 (the first and last measurement on the 1^{st} night) were removed because of their large errors with respect to the fit, as were five further points from Run 2 (last measurement on 2^{d} night), and four that were contaminated by a field star (21 Oct. 1997). It should be noted that the error bars in Fig. 3 include the photometric calibration (which has a systematic component for each night) as well as the photon noise. Most of the systematic error is removed in the period searching program by resetting the zero point of the magnitude scale each night. For this reason, the dispersion of the points with respect to the fit is smaller than would be expected from the error bars.

As the amplitude of the resulting lightcurve is quite large compared to the photometric error (which include both the absolute error of the photometric equations and the photon noise), as the measured variations are much larger than the residual variations of stars of similar brightness (which represent the photon noise and the errors of the relative photometry correction – cf. Fig. 1), because the deduced 6.25h period does not correspond to any of the sampling periods, and since the same and only period fits the data of both observation runs, there is little doubt that the phased lightcurve represents the physical rotation of the object.

The lightcurves from Runs 1 and 2 are consistent and have an almost perfectly symmetrical double-peak, typical of a shape-dominated lightcurve, with a peak-to-peak amplitude of 0.12 mag. Assuming that 1996 TO_{66} can be modeled by a tri-axial ellipsoid with no albedo feature (a realistic possibility considering the shape of the lightcurve; let $a > b > c$ be the three semi-major axis), a lower limit for the elongation (ϵ) may be estimated as:

$$\epsilon = a/b \geq 10^{0.4\Delta m} \quad (1)$$

$$\geq 1.12. \quad (2)$$

i.e. an elongation of 12% or more. This result, combined with the radii obtained in the previous section and with the rotation period obtained for 1996 TO_{66}, is not giving useful constraints on the density nor internal cohesion of the object.

Soon after the analysis of the data from Runs 1 and 2 was done, additional data were obtained from Run 3. Because of the visibility of the object at that time and of other scheduling constraints, the coverage of the lightcurve during Run 3 is not optimal for a period search; indeed all data were obtained during an interval of only ∼3h each night. The algorithm found $P_{\rm syn} = 6.25$ h and 9.7h to be the best fitting periods. Re-phasing the data with the latter period leads to a double-peaked lightcurve, while the former gives a single-peaked lightcurve. An attempt to rephase the data from Run 1 and 2 with the 9.7h period failed: the resulting lightcurve gives a very bad fit to the data (*eg* , the ascending part of the lightcurve from one night overlaps with the descending part from another). It is therefore highly likely that the real rotation period of 1996 TO_{66} is 6.25h; the data from Run 3, folded with this period, are presented at Fig. 3.

In addition to the single-peaked shape, the lightcurve from Run 3 has a peak-to-peak amplitude of 0.33 mag, *i.e.* 2.5 times larger than the amplitude measured during Runs 1 and 2. Several hypotheses will now be considered to explain this changes of shape and amplitude of the lightcurves between the 1997 and 1998 observation runs.

3.3.2. Discussion

Even though the observations were performed over a period of one year, the change of the object's ecliptic longitude is small, from 358.3° to 359.7°. Therefore, if it is assumed that the rotation is simple (*i.e.* no tumbling), the change of aspect angle (the angle between the line of sight and the rotation axis) between the epochs is negligible, and certainly cannot explain the observed change of lightcurve amplitude (Detal et al. 1994). This effect can therefore have been caused either by *i)* a change of aspect resulting from a complex rotation, or *ii)* by some physical changes of 1996 TO_{66} itself.

Complex Rotation: Let us first consider the hypothesis of a complex rotation in which the object is rotating with a principal period of 6.25h, overlaid by a large precession with a period of the order of several months, long compared to one run, but comparable to the time between Runs 1 and 3. Burns & Safronov (1973) studied the theoretical aspects of complex rotation of tumbling asteroids in detail. They quantified τ, the damping time scale of a complex rotation as

$$\tau \sim \mu Q/(\rho K_3^2\, r^2 \omega^3), \quad (3)$$

where μ is the rigidity of the material of which the asteroid is composed, Q is the ratio of the energy contained in the oscillation to that lost per rotation, ρ is the density of the object, K_3^2 quantifies the irregularity of the body (from 0.01 for nearly spherical to 0.1 for highly elongated), r is the mean radius of the object, and ω the angular frequency of rotation. Their main result is that the damping time scale of complex rotation is short compared to the other time scales involved (like the mean time interval between collisions, which would re-excite a complex rotational state), and therefore that all asteroids should be in a simple rotation about their axis of maximum inertia. However, Harris (1994) revisited their results in the light of more recent observations and reached the conclusion that tumbling *is* possible for small objects with slow rotation. Using his estimations, the damping time scale for an object like 1996 TO_{66} is found of the order of 100 yrs, thus making a complex rotation extremely unlikely. Of course, Harris' parameters were chosen to represent main belt asteroids. Nevertheless, even changing the value of μ and ρ (the parameters that are most likely to be different for a TNO), τ will not be changed by the many orders of magnitude needed to make plausible a complex rotation of 1996 TO_{66}. Samarasinha & Belton (1995) have studied in detail the rotational state of cometary nuclei, and found that the change in rotational state of a nucleus strongly depends on the location and strength of the active areas on the surface. Even considering that 1996 TO_{66} is active (cf below), maintaining it in a tumbling state would require very strong and concentrated jets with a very specific surface configuration; we consider this very unlikely.

Let us nevertheless consider the implications of 1996 TO_{66} being in a state of complex rotation. The lightcurve amplitude was the same during Runs 1 and 2, suggesting that the aspect angle of the asteroid did not change between the runs. This is further confirmed by additional observations, kindly made available by Tegler and Romanishin (private communication), that were obtained at an epoch intermediate between Runs 1 and 2. While their data are too sparse to permit an independent study, they are compatible in magnitude and amplitude with the data from Runs 1 and 2. It should however be noted that they

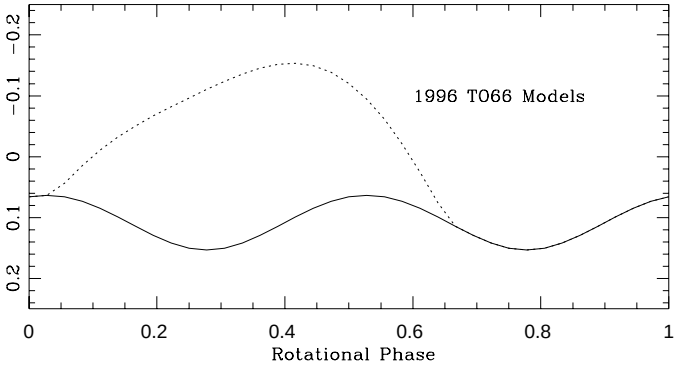

Fig. 4. Model lightcurves of 1996 TO_{66}. The solid curve represents an ellipsoid (a=1.2; b=c=1; aspect angle A=45°) of uniform albedo (0.04), and the dotted line the effect of a 60 km radius spot of albedo 0.45. While many models reproduce the observed lightcurves, this one was chosen for its very conservative parameters, c.f. the text.

do not see an evidence of the lightcurve we report here, but a 0.12 mag amplitude would be a 2σ detection (priv. communication). The precession period must therefore be significantly larger than 2 months (interval between Runs 1 and 2), but of the order of $\sim$ 1 yr (interval between Runs 2 and 3). Moreover, as the lightcurves of Runs 1/2 and 3 are very different, the precession angle must be large enough to cause a large change of aspect angle. Finally, in order to explain the one-peaked appearance of the Run 3 lightcurve, the object must have either a very complex shape (including significant, large-scale concavity to give the one-peaked lightcurve) and/or a significant albedo marking (Russell 1906), that is visible with the Run 3 geometry, but not with that of Runs 1/2. In summary, considering the implied, very short complex rotation damping time scale, the very strict requirements on the precession period and the unusual topology of the object, we consider that this hypothesis is unlikely.

Collision: We now explore the possibility of 1996 TO_{66} having a stable rotation axis, but that a significant change occurred on the surface of the object between Runs 1/2 and 3. During the first two runs, 1996 TO_{66} exhibited a lightcurve typical of a slightly elongated object with a uniform albedo, in agreement which what would be expected for a large TNO. During Run 3, the larger amplitude, single-peaked lightcurve suggests either a quite elongated body with significant concavity or a spot of brighter albedo. A collision with a large body would be required to produce the drastic change of shape required. Stern (1995) extensively studied the time scales for collisions in the Kuiper Belt; according to his simulations, the time scale for collisions with a large object (*i.e.* involving sufficient energy to significantly change the shape of 1996 TO_{66}) is much larger than the age of the Solar System. It is therefore extremely unlikely that such a dramatic event happened between October 1997 and September 1998. We therefore now consider the possibility that the peculiar shape of the lightcurve observed during Run 3 is caused by a spot with an albedo that differs from that of the rest of the surface.

Bright Spot: In order to quantify the requirements on an albedo spot for reproducing the observed lightcurve, a simple modeling of the lightcurve was performed. A bi-axial ellipsoid of uniform albedo was chosen to reproduce the Run 1/2 lightcurves, and a spot of higher albedo was added to reproduce the Run 3 data. *Many* models exist that satisfy these conditions. As an example, Fig. 4 displays the corresponding lightcurves for a model with very conservative parameters, ellipsoid axis ratio $a/c = 1.2, b/c = 1$, aspect angle $A = 45°$, relative radius of the spot $r/c = 0.21$, albedo of the spot $p_s = 0.45$ (the remainder of the surface having $p = 0.04$), position of the spot: latitude 20°, longitude 65°(the origin of longitude being the long axis of the object). For this model, which will be used as basis for the following discussion, the global albedo was thus set to the typical value for distant minor bodies, while that of the spot corresponds to a value intermediate between the albedoes of Pluto and Charon, 0.6 and 0.3 resp., cf. Albrecht et al. (1994). It should be noted that the observed lightcurves can also be reproduced by a brighter object with albedo $p = 0.35$ and a larger spot ($r/c = 0.8$, *i.e.* covering almost one complete hemisphere) of albedo $p_s = 0.65$. The size of the spot also depends on its position; for instance, a partially hidden spot can be much larger without changing the resulting lightcurve. This exercise showed that the observed lightcurve is quite easy to reproduce with a spot of reasonable size and albedo.

If we assume that the surface was originally completely covered by a crust of low albedo, then such a bright spot could have been generated by removing a part of this crust, thereby exposing the underlying, fresh ice of higher albedo. This might be caused either by a collision with a small object, or by intrinsic (cometary) activity.

The hypothesis of the bright spot is further supported by the brightening of 1996 TO_{66} (in absolute mag.) between Runs 1/2 and 3 (cf. Sect. 3.1 and Table 4): the difference of average magnitude between the models with a spot and without a spot perfectly matches this brightening. We also listed in Table 4 the results published by Romanishin & Tegler (Romanishin & Tegler 1999) and Jewitt & Luu (Jewitt & Luu 1998), as a comparison.

We first consider an impact. Weissman & Stern (1994) studied the cratering of Pluto and Charon using the results of Holsapple (1993); assuming that their analysis can be directly scaled to 1996 TO_{66}, the diameter of the impactor causing the bright spot of the above model is given by

$$d = (D/1.26\ A^{-1/3}\ (1.61g/v_i^2)^{\alpha/3})^{1/(1-\alpha/3)}, \quad (4)$$

where D is the diameter of 1996 TO_{66}, g the surface gravity of the target, A and α are constants that depend on the mechanical properties of the target surface material, v_i is the impactor velocity (we used 0.2, 0.6, and 1.7 km/s, respectively, as did Weissman & Stern (1994) for impactors from the outer Solar System on Pluto/Charon). With these values, the bright spot could have been caused by the impact of an object of $\sim$ 20km diameter. Again using the results of Stern's (1995) simulations, such collisions have a time scale of a $1 - 5 \times 10^9$ years (depending on the orbit distribution used); again, the *a priory* probability

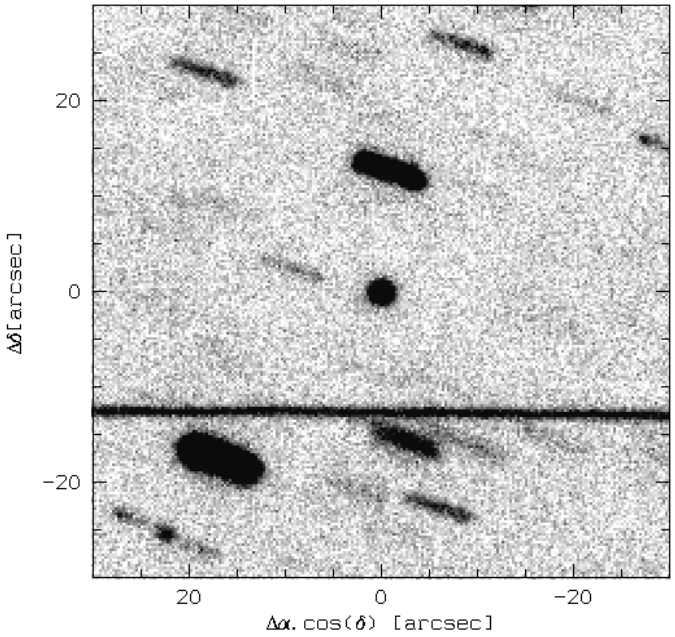

Fig. 5. Composite of 15 R images of 1996 TO_{66}, totaling 13,500s exposure time. The individual frames were selected from Run 2, for being taken when the sky was photometric and the object was not too close to any field star. The horizontal line is the trail of an artificial satellite.

for such an event happening between Runs 2 and 3 is therefore extremely low.

Finally, the bright spot reproducing the lightcurves could also have been produced by removing the dark crust by surface (cometary) activity, exposing underlying fresh and brighter ice. In the case of the Centaur (2060) Chiron, that is probably very similar to the TNOs, a (cometary-type) coma has been detected (Meech & Belton 1989), and was continuously monitored since then. Chiron even displayed a tail in 1992–1993. More recent, high-resolution images have shown that part of this coma is gravitationally bound to the object (Meech et al. 1997). Such a coma is extremely efficient in covering the surface with fresh material. Additionally, short and violent activity outbursts, originating from isolated regions of the nucleus have been observed in comets at large heliocentric distances, e.g. in Comet C/1995 O1 (Hale-Bopp) at $r = 7.5$ AU (Boehnhardt et al. , in preparation), or in Comet 1P/Halley at 14.5 AU (West et al. 1991). Activity has also been detected at much larger heliocentric distances, for instance in Comet C/1987 H1 (Shoemaker) that still had a large tail at 23.75 AU (Meech et al. 2000); simulations showed that the dust composing this tail could not have been the remnant of an activity at small heliocentric distances. A possible $(2-3\sigma)$ high-resolution HST detection of a coma around the TNO 1994 TB has been recently reported (Fletcher et al. 2000), when this object was at $r = 30$ AU.

While these observations demonstrate that cometary activity is possible at very large heliocentric distances, one of the major questions inherent to this scenario is that of the nature of a volatile species that may cause such activity at the low ambient temperature. N_2, CO and CH_4 are suspected components of the TNOs, and they are known to play a role in Pluto's atmosphere, which is continuously replenished by sublimation (and could thus be considered as an extreme case of cometary activity). However, while CO can sublimate at the distance of 1996 TO_{66}, laboratory experiments with condensation of water ice at low temperature show that CO will not condense as an ice, but rather will be trapped as a gas in the water ice matrix. In that case, it is not expected to cause activity at this distance (Bar-Nun & Owen 1998). In summary, while the underlying physical causes of cometary activity at large heliocentric distances are not yet understood, clear observational evidence exists for such activity and it is therefore a possible explanation for the formation of a bright spot on the surface of 1996 TO_{66}.

Interestingly, Brown et al. (1999) have observed 1996 TO_{66} with the Keck telescope during our Run 3. They published two near-IR spectra that display clear absorption lines from water. From the ratio between some of these lines, they conclude that one side of the object is dominated by amorphous ice, while the other is covered with crystalline ice. It is interesting to note that this observation is compatible with our interpretation of the lightcurve change. Indeed, the surface should be covered mostly with old ice, which would have had time to undergo the amorphous to crystalline transformation, while the active side is expected to have a spot where deeper material is exposed, which is more likely to contain some amorphous ice. This should be confirmed by a comparison of the rotational phase at which the spectra were obtained.

3.4. Photometric profile

In order to further investigate the possibility that 1996 TO_{66} possesses cometary activity, the R frames obtained at Run 2 and Run 3 during photometric sky conditions and when the object was not too close to a field star, were registered on 1996 TO_{66} and co-added. Part of the resulting frame for Run 2, totaling 13,500s exposure time on the NTT, is displayed in Fig. 5. The image quality measured on this composite is $1\farcs06$ FWHM. The composite of Run 3 images totals 4500s on the UH 2.2m, and is $0\farcs65$ FWHM. Photometric profiles have been extracted from these images, by integrating the light in narrow annuli (1/2 original pixel wide) centered on the object. Images were also registered on field stars and co-added, resulting in a stacked frame on which the images of stars have the same image quality (FWHM) as that of the first stack. Photometric profiles were extracted from several field stars. They were normalized to the same intensity as that of the object and averaged, providing a Point Spread Function (PSF) for comparison. Fig. 6 displays both profiles for both runs, and shows that the profile of the TNO matches that of the PSF, up to the radius at which at which the former is dominated by noise. We conclude that no resolved coma is detected.

For an un-trailed object with no coma (e.g. 1996 TO_{66}), the subtraction of the normalized stellar profile fluxes from those of the object should yield a value of zero with an associated error.

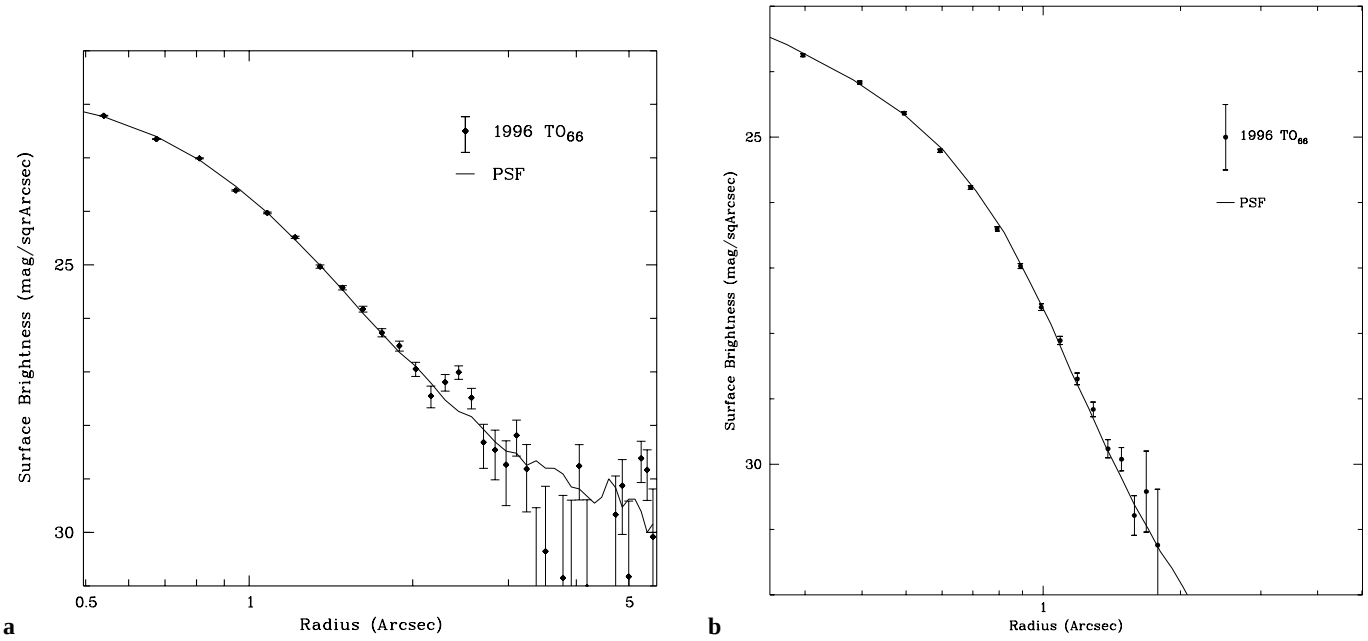

Fig. 6a and b. Photometric profiles of 1996 TO_{66} (solid circles), **a** from Run 2 (13,500s, NTT) extracted from the image shown in Fig. 5, and **b** from Run 3 (4,500s, UH 2.2m), compared to an average PSF. No coma is seen

One can use 3σ of this error as the limiting possible maximum flux contributed from scattered coma light.

Assuming that the coma is not affected by the gravitation of the object (*i.e.* neglecting a possible bound coma), this flux will be given by:

$$F = S_{\odot}\pi a_{\rm gr}^2 p_v Q\phi/2r^2\Delta^2 v_{\rm gr} \quad (5)$$

where $S_{\odot}$ is the solar flux through the bandpass [W m^{-2}], $a_{\rm gr}$ [m] the grain radius, p_v the grain albedo, Q [particle s^{-1}] the dust production rate, ϕ the projected size of the aperture [m], $v_{\rm gr}$ [m s^{-1}] the grain velocity, and r and Δ the helio- and geocentric distances. It should be noted, that if one assumes a Bobrovnikoff relation for the terminal grain velocities, $v_{\rm gr} = v_{\rm bob} = 600\ r^{-0.5}$, that for a given observed flux, the dust production will vary as

$$Q \propto r^{1.5}\Delta^1, \quad (6)$$

such that the most sensitive limits will be made when the object is observed at the smallest heliocentric distance.

Using Eq. (5), and using the 3σ errors of both the PSF and object profiles added in quadrature ($3F_{\rm err}$), we computed the upper limit to the total production rate as a function of the coma radius with

$$Q \leq \frac{2(3F_{\rm err})\Delta r^2 v_{\rm gr}}{S_{\odot}\pi a {\rm gr}^2 p_v \phi}. \quad (7)$$

With a seeing near 0.″65, the most sensitive upper limits for dust mass loss for 1996 TO_{66} must be obtained outside the seeing disk, near 0.″8–1.″0 at $Q = 0.03 - 0.05$kg sec^{-1}. This is nearly 2 orders of magnitude less than the activity seen for low activity comets. In this computation, we take into account only the gravitationally free coma, not the gravitationally bound coma that could exist around 1996 TO_{66}, which is much bigger than Chiron, which displays a bound coma (Meech et al. 1997).

As mentioned above, Fletcher et al. (2000) have reported the detection with the HST of a coma around the TNO 1994 TB at a surface brightness deviation of 0.5mag/sq.arcsec. (corresponding to a $2-3\sigma$ detection) at 0.2–0.″5 from the nucleus. At that distance from the center, the present profile of 1996 TO_{66} is still completely dominated by the seeing disk of the nucleus. Assuming that 1996 TO_{66} is surrounded by a coma similar to that of 1994 TB in terms of surface brightness and with steady state expansion $1/\rho$ profile (*i.e.* assuming that it is not a bound coma), this would result in an excess of 25 to 26 mag/sq.arcsec at $\rho = 0.8$ and 2″, respectively, *i.e.* , it would have been easily detected.

Brown & Luu (1998) performed some Monte-Carlo simulations of the life-time of comae around various template TNOs, including 1996 TO_{66} (although the preliminary radius they used for this object is different from ours). They determined that an outburst creating a Chiron-like coma around 1996 TO_{66} would *not* have been detectable, and that a coma 10 times as massive as that of Chiron would have been visible for 40 days before becoming too dispersed. Although their criteria for detectability were based on a total brightness excess, their coma dispersion time-scale is compatible with the assumption that 1996 TO_{66} experienced an outburst between Runs 2 and 3 that created the surface spot and the fact that no coma was observed during Run 3.

3.5. Spectrum

The resulting 8100s spectrum of 1996 TO_{66} is presented in Fig. 7 as a reflectance spectrum obtained from division with the spectrum of the solar analog.

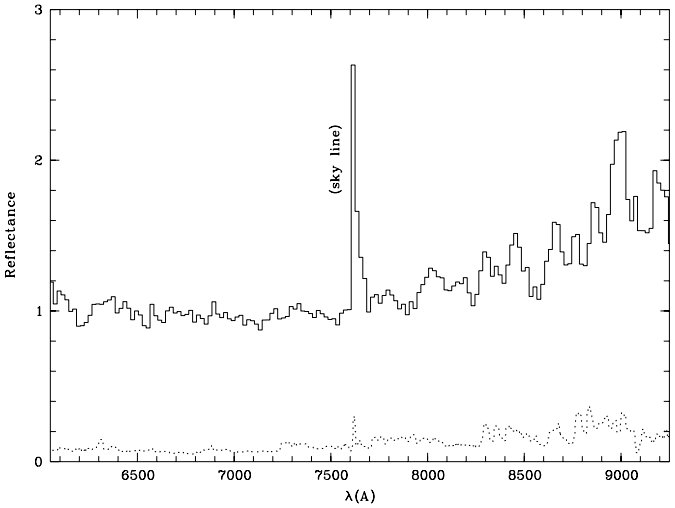

Fig. 7. Reflectance spectrum of 1996 TO_{66} (top, solid line), obtained by dividing the composite spectrum of the object (totaling 8100s exposure with the NTT and EMMI/RILD on Oct. 25, 1997) by that of the solar analog, normalized at 6410Å. The spectrum has been median filtered with a window of 5 pix (13Å) and rebinned to 20Å pixels. The dotted line represents the noise level (obtained from the sky photon noise). A proeminent sky absorption line (appearing as a peak in this ratio) is marked. No obvious spectral features are seen.

The extracted spectrum of 1996 TO_{66} was quite noisy and has been smoothed by means of a sliding median filter with a window of 5 pixels (~ 13Å). The original noise level is shown on the figure; the signal-to-noise ratio is of the order of S/N ~ 10, depending on the wavelength. Except for a strong telluric absorption line (marked on the figure), the spectrum is featureless, with a neutral colour in the lower wavelength range ($S' = 0. \pm 5.$%/1000Å), then a small but significant red gradient ($S' = 30. \pm 10$%/1000Å) in the 8,000–9,000Å range, *i.e.* beyond the range accessed by broad-band photometry. The gradients measured in the R–I wavelength range can be converted into $R - I = 0.35 \pm 0.05$ (cf. Davies et al. 1997), which is in good agreement with the color obtained in Sect. 3.2. It should be noted that such change of gradient in the reflectivity spectrum of a Solar System object has never been observed before, and should be confirmed with independent observations.

Although the spectrum does not reveal any feature, it shows that data obtained on a 4m-class telescope can give useful S/N ratio if carefully processed.

4. Conclusions

1996 TO_{66} was observed with the ESO 3.6m NTT (Aug. and Oct. 1997) and the UH 2.2m (Sep. 1998) telescopes. The main results of these observations are the following:

– The mean magnitude of 1996 TO_{66} is converted into a radius of ~ 320km, assuming a standard albedo of 0.04.

– The colours of 1996 TO_{66} are grey-blue, making it the bluest TNO known to date.

– An apparently featureless 8100s spectrum of low S/N ratio (~ 10) has a spectral gradient of $S' = 0 \pm 5$%/1000Åin the 6,300–7,500Åregion, and $S' = 30 \pm 10$%/1000Åin 8,000–9,000Å.

– The rotational period of 1996 TO_{66} is $P_{\rm syn} = 6.25 \pm 0.03$h. The amplitude of the 1997 lightcurve corresponds to an elongation $\epsilon \geq 1.12$.

– The amplitude and morphology of the 1998 lightcurves are completely different from those obtained in 1997. We discuss possible origins for this change. Complex rotation and an impact are unlikely because of the time-scale of these phenomena. We conclude that the effect is most likely due to the apparition of a bright spot caused by a short, localized "cometary activity" outburst, which has covered a small part of the surface with fresh material of higher albedo.

– We do not detect a coma around the object. However, this is not surprising, considering the small size and short life-time expected for such a coma.

The grey-blue colour of the surface of 1996 TO_{66} , and the probable outburst provide a coherent picture of this object. Indeed, if such outbursts are common and frequent resurfacing takes place, the surface material may not have time to become tholin-like by photo-degradation.

Considering the very long time-scale for collisions among 1996 TO_{66}-like objects indicated by Monte-Carlo simulations, and that two of the very few TNOs which have been thoroughly observed (1994 TB and 1996 TO_{66}) are suspected to harbour "cometary" activity, it may well be that this phenomena is quite common in the Kuiper Belt. This would then provide an alternative to collisions for explaining the large colour range observed among TNOs, that are expected to become redder whenever they remain undisturbed over long periods. If confirmed, this possibility may force us to reconsider the TNO formation scenario, since volatiles that condensed with water at very low temperature are embedded within the water ice and thus are not expected to contribute to cometary activity (Bar-Nun & Owen 1998). This may then indicate that the TNOs have undergone important structural changes after their formation, as also suggested by Prialnik (2000).

Acknowledgements. We are very grateful to S. Tegler and W. Romanishin, who kindly sent us their unpublished 1996 TO_{66} data; to S. Tegler who, as referee, gave us valuable advises to improve this paper, and to L. Jorda, who made available to us some of his neat software. Support for this work was provided to KJM and JB by NASA Grant No. NAG5-4495.

References

Albrecht R., Barbieri C., Adorf H.-M., et al., 1994, Astrophys. J. 435, L75

Bar-Nun A., Owen T., 1998, In: Schmidt B., De Berg C., Festou M. (eds.) Solar System Ices, p. 353, Kluwer, the Netherlands

Barucci M.-A., Doressoundiram A., Tholen D., Fulchignoni M., 1999, Icarus, in press

Böhnhardt H., Hainaut O.R., Delahodde C.E., et al., 2000, In: Fitzsimmons A. (ed.) Minor Bodies in the Outer Solar System, (Ed.), ESO, in press

Böhnhardt H., Rainer N., Birkle K., Schwehm G., 1999, Astron. Astrophys. 341, 912–917

Bowell E., Hapke B., Domingue D., et al., 1989, Binzel R.P., Gehrels T., Matthews M.S. (eds.) Asteroids, pp. 524–556, Univ. AZ Press
Brown H., Cruikshank P.D., Pendleton Y., Weeder, G.J., 1997, Science 276, 937
Brown R.H., Cruikshank D.P., Pendleton Y., 1999, Astrophys. J. 519, L101
Brown W.R., Luu J.X., 1998, Icarus 135, 415
Burns J.A., Safronov V.S., 1973, Mon. Not. R. Astron. Soc. 165, 403
Davies J.K., 2000, In: Fitzsimmons A. (ed.) Minor Bodies in the Outer Solar System, ESO, in press
Davies J.K., McBride N., Green, S.F., 1997, Icarus 125, 61
Davis D.R., Farinella P., 1997, Icarus 125, 50
Delahodde C.E., Hainaut O.R., Böhnhardt H., 2000, In Asteroids Comets Meteors in preparation
Detal A., Hainaut O.R., Pospieszalska-Surdej A., et al., 1994, Astron. Astrophys. 281, 269
Edgeworth K., 1943, J. Br. Astron. Assoc. 53, 181
Farinella P., Davis D.R., 1996, Science 273, 938
Fletcher E., Fitzsimmons A., Williams I.P., Thomas N., Ip, W.-H., 2000, In: Fitzsimmons A. (ed.) Minor Bodies in the Outer Solar System, ESO, in press
Hainaut O.R., Meech K.J., Böhnhardt H., West R.M., 1998, Astron. Astrophys. 333, 746
Hamuy M., Suntzeff N.B., Heathcote S.R., et al., 1994, Publ. Astron. Soc. Pac. 106, 566
Hamuy M., Walker A.R., Suntzeff N.B., et al., 1992, Publ. Astron. Soc. Pac. 104, 533
Harris A.W., 1994, Icarus 107, 209
Harris A.W., Lupishko D.F., 1989, In: Binzel R., Gehrels T., Matthews M. (eds.) Asteroids II, pp. 39–53, University of Arizona, Tucson
Holsapple K.A., 1993, Annu. Rev. Earth Plan. Sci. 21, 333
Jewitt D.C., 2000, In: Fitzsimmons A. (ed.) Minor Bodies in the Outer Solar System, ESO, in press
Jewitt D.C., Luu J.X., 1992, IAU Circ. 5611
Jewitt D.C., Luu J.X., 1998, Astron. J. 115, 1667
Johnson R.E., Cooper J.F., Larenzotti L.J., Strazzulla G., 1987, Astron. Astrophys. 187, 889
Kalas P., 2000, In: Alloin D. (ed.) VLT Opening Symposium, in press
Kuiper G., 1951, In: Hynek J. (ed.) Astrophysics: A total Symposium, pp. 357–424, McGraw-Hill, New York
Landolt A., 1992, Astrophys. J. 104, 340
Luu J.X., Jewitt D.C., 1990, Icarus 86, 69
Luu J.X., Jewitt D.C., 1996, Astron. J. 111, 499
Luu J.X., Jewitt D.C., 1998, Astrophys. J. 494, L117
Luu J.X., Marsden B.G., Jewitt D.C., et al., 1997, Nature 387, 573
Malhotra R., 1996, Astron. J. 111, 504
Malhotra R., 1997, Bull. Am. Astron. Soc. 29, 1016
McCaughrean M., 2000, In: Alloin D. (ed.) VLT Opening Symposium in press
Meech K.J., Belton M.J.S., 1989, IAU Circ. 4770
Meech K.J., Buie M.W., Samarasinha N.H., Mueller B.E.A., Belton M.J.S., 1997, Astron. J. 113, 844
Meech K.J., Hainaut O.R., 1997, IAU Joint Discussion on Interaction between Planets and Small Bodies, Kyoto, Aug. 1997
Meech K.J., Hainaut O.R., Marsden B.G., 2000, In: Fitzsimmons A. (ed.) Minor Bodies in the Outer Solar System, ESO, in press
Moroz L., Arnols G., Korochantsev A.V., Wasch R., 1998, Icarus 134, 253
Prialnik D.A., 2000, In: Fitzsimmons A. (ed.) Minor Bodies in the Outer Solar System, in press
Prialnik D.A., Bar-Nun A., 1990, Astrophys. J. 355, 281
Prialnik D.A., Bar-Nun A., Podokal M., 1987, Astrophys. J. 319, 993
Romanishin W., Tegler S., 1999, In: Exploring the Kuiper Belt, Lowell Observatory
Romanishin W., Tegler S., 1999, Nature 398, 129
Russell H.N., 1906, Astrophys. J. 24, 1
Russell H.N., 1916, Astrophys. J. 43, 173
Sagan C., Khare B.N., Lewis J.S., 1984, In: Matthews M., Gehrels T. (eds.) Saturn, pp. 788–807, University of Arizona Press, Tucson
Samarasinha N.H., Belton M.J.S., 1995, Icarus 116, 340
Stern S.A., 1995, Astron. J. 110, 856
Stern S.A., 1996, Astron. J. 112, 1203
Tegler S.C., Romanishin W., 1998, Nature 392, 49
Thomas N., Eggers S., Ip W.-H., et al., 2000, In: Fitzsimmons A. (ed.) Minor Bodies in the Outer Solar System, ESO, in press
Trujillo C., 2000, In: Fitzsimmons A. (ed.) Minor Bodies in the Outer Solar System, ESO, in press
Weissman P.R., Stern S.A., 1994, Icarus 111, 378
West R.M., Hainaut O.R., Smette A., 1991, Astron. Astrophys. 246, L77

Note added in Proofs. Recent VLT observations confirm the larger amplitude and single peak of the light curve, but do not confirm the red gradient in the spectrum.